Transbilayer Movement and Net Flux of Cholesterol and Cholesterol Sulfate between Liposomal Membranes

Wendi V. Rodrigueza,[‡] Jeffery J. Wheeler,[§,||] Sandra K. Klimuk,[‡] C. Neil Kitson,[‡] and Michael J. Hope*[,‡,||]

Liposome Research Unit, University of British Columbia, Vancouver, British Columbia, Canada V6T 1Z3

Received November 11, 1994; Revised Manuscript Received February 14, 1995[⊗]

ABSTRACT: The kinetics of cholesterol and cholesterol sulfate (CS) movement between vesicles have been investigated. CS is widely distributed in cell membranes, plasma, and skin and is similar in structure to cholesterol, but possesses an ionizable sulfate moiety at the 3β-position which imparts a negative charge at physiological pHs. Donor vesicles of various sizes ranging from 40 to 250 nm, composed of egg phosphatidylcholine (EPC)/sterol/*N*-palmitoyldihydrolactosylcerebroside (75:10:15 mole ratio) containing trace amounts of [^{3}H]sterol, were used to monitor sterol transfer into a 10-fold excess of large unilamellar vesicles (LUV) composed of EPC with a diameter of 100 nm. The two populations of vesicles were separated by centrifugation following the addition of a lectin which caused the aggregation of donor vesicles. Both cholesterol and CS exhibited biphasic kinetics of exchange. The rate constants for efflux and transbilayer diffusion for both sterol molecules were determined after fitting kinetic data, using numerical integration, to a three-compartment model, which includes the inner and outer monolayers of donor vesicles and the acceptor bilayer. The rate of intermembrane exchange for CS was approximately 10-fold faster than for cholesterol in all liposomes tested. Using the kinetic model, a rate of transbilayer movement for cholesterol and CS was estimated. In both cases, it was found to be slower than the rate of efflux from the surface of vesicles. For vesicles containing CS, the surface charge was monitored to demonstrate that the slowly exchanging pool was located in the inner monolayer, and the rapidly exchanging pool in the outer half of the bilayer. For cholesterol, it was not possible to distinguish between this model and one where lateral domains of cholesterol within the plane of the bilayer may influence the kinetics of exchange.

The movement of cholesterol between various liposomal systems has been measured and compared to cholesterol sulfate, which is less abundant than cholesterol, but widely distributed in plasma membranes, lipoproteins, and skin (Bleau et al., 1974). The reasons for comparing the kinetics of cholesterol sulfate (CS)[1] exchange and net flux to those of cholesterol are 2-fold. First, there are several models describing the exchange kinetics observed for cholesterol, and in model membranes, it is not clear whether transbilayer movement is rate-limiting when considering the net efflux of sterol from a donor bilayer to excess acceptor. This is partly the result of conflicting data in the literature concerning the rate of cholesterol flip-flop [reviewed in Schroeder and Nemecz (1990)]. Cholesterol sulfate, on the other hand, contains a negatively charged sulfate moiety (see Figure 1), which should reduce the energy required for this sterol to desorb from a bilayer surface and therefore enhance the flux from donor to acceptor membranes compared to cholesterol. However, the negative charge can also be expected to inhibit transbilayer movement, owing to the increased energy required to move it through the hydrophobic interior of the membrane (Hope & Cullis, 1987; Hope et al., 1989b; Kan et al., 1992). Consequently, one should observe a clear separation between the kinetics of intermembrane exchange and transbilayer diffusion, in contrast to that observed for neutral cholesterol. Furthermore, the negative surface charge can be monitored and correlated with the loss of CS from the outer monolayer of donor membranes. Second, although quantitatively less important than cholesterol, the sulfate derivative is found in erythrocytes, sperm, and myelin membranes (Bleau et al., 1974) as well as epidermis (Wertz, 1992). The physiological role of this molecule remains unclear, and to our knowledge, there are no published studies comparing the exchange kinetics of CS to those of cholesterol in model membranes. Examining the dynamics of CS in model membranes may help determine a biological function for this interesting molecule as well as help us better understand the exchange kinetics of cholesterol itself. Consequently, in this investigation we have employed well-defined, unilamellar vesicles as well as multilamellar systems

* Address correspondence to this author at Inex Pharmaceuticals Corp., 1779 W. 75th Ave., Vancouver, British Columbia, Canada V6P 6P2.

‡ Also at the Skin Barrier Research Laboratory, Department of Medicine, University of British Columbia, Vancouver, British Columbia.

§ Also at the British Columbia Cancer Control Agency, Vancouver, British Columbia.

|| Also at Inex Pharmaceuticals Corp., 1779 W. 75th Ave., Vancouver, British Columbia V6P 6P2.

⊗ Abstract published in *Advance ACS Abstracts,* April 1, 1995.

[1] Abbreviations: Cer, cerebroside; CHE, cholesteryl hexadecyl ether; C:P, cholesterol-to-phospholipid ratio; CS, cholesterol sulfate; DSPG, distearoylphosphatidylglycerol; EPC, egg phosphatidylcholine; HBS, HEPES-buffered saline; HEPES, 4-(2-hydroxyethyl)]-1-piperazineethanesulfonic acid; IM, inner monolayer; k_1, rate constant for transbilayer diffusion of sterol; k_2, rate constant for intermembrane sterol exchange; LUV, large unilamellar vesicle(s); LUV_{100}, LUV extruded through 100 nm pore size polycarbonate filters; MLV, multilamellar vesicle(s); MLV_{400}, MLV extruded through 400 nm pore size polycarbonate filters; NaCl, sodium chloride; NMR, nuclear magnetic resonance; OM, outer monolayer; PC, phosphatidylcholine; SUV, small unilamellar vesicle(s); $t_{1/2}$, half-times; $t_{1/2,flip}$, half-times of flip-flop; $t_{1/2,exc}$, half-times of intermembrane exchange.

0006-2960/95/0434-6208$09.00/0

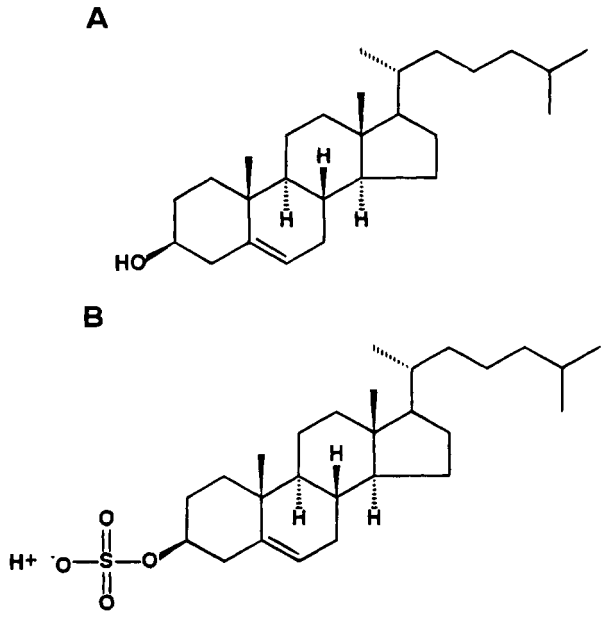

FIGURE 1: Structure of cholesterol and cholesterol sulfate.

to measure the intermembrane movement of sterol under nonequilibrium conditions, chosen to promote net depletion from donor membranes.

MATERIALS AND METHODS

Materials. [1,2-^{3}H]Cholesterol, [*cholesteryl*-1,2-^{3}H(N)]-cholesteryl hexadecyl ether ([^{3}H]CHE), and [^{14}C]cholesteryl hexadecyl ether ([^{14}C]CHE) were obtained from Du Pont New England Nuclear (Boston, MA). [1,2-^{3}H]Cholesterol sulfate was prepared as described below. Egg phosphatidylcholine was purchased from Princeton Lipids (Princeton, NJ) and distearoylphosphatidylglycerol (DSPG) from Avanti Polar Lipids (Birmingham, AL). Cholesterol, cholesterol sulfate (CS), *N*-palmitoyldihydrolactocerebroside (Cer), the galactosyl-binding lectin from *Ricinus communis* (RCA-120), 4-(2-hydroxyethyl)-1-piperazineethanesulfonic acid (HEPES), and DEAE-Sepharose CL-6B were obtained from Sigma Chemical Co. All solvents, chemicals, and thin-layer silica chromatography plates were of analytical grade and were from BDH Chemicals (Vancouver, B.C.).

Synthesis of [1,2-^{3}H]Cholesterol Sulfate from [1,2-^{3}H]-Cholesterol. [1,2-^{3}H]Cholesterol sulfate was synthesized from [1,2-^{3}H]cholesterol (specific activity 58 Ci/mmol) according to the method described by Williams et al. (1983) with the following modifications. Briefly, radiolabeled cholesterol dissolved in ethanol was dried down, mixed with a 100-fold excess of sulfamic acid in 2 mL of dry pyridine in a 16 × 100 pyrex tube, and heated at 95−100 °C for 2 h in a boiling water bath. A parallel reaction with unlabeled cholesterol was also carried out. After the reaction mixture had cooled, 10 mL of methanol was added to extract the lipids from unreacted sulfamic acid and was placed in a round-bottom flask. Two additional methanol extractions were performed, and the solvents were removed by evaporation. Subsequently, approximately 20 mL of toluene was added to the flask to aid the removal of any remaining pyridine. CS was purified by preparative thin-layer chromatography (TLC) using ether/methanol/ammonium hydroxide (9:1.3:0.4 v/v) as running solvent. The area of the plate which comigrated with the CS standard was extracted with benzene/methanol (70:30 v/v). The sodium salt of CS was generated by solubilizing the dry lipid film with an acidified distilled water−hydrochloric acid (pH 2)/chloroform/methanol (1:1:2.1 v/v) solution. The pH of this one-phase mixture was raised to 7 by titration with NaOH. Thereafter, CS was extracted from the lower phase of the mixture following the addition of the appropriate amounts of 400 mM NaCl and chloroform to generate two phases according to the Bligh and Dyer (1959) procedure.

Table 1: Vesicle Preparations Used in Sterol Flux Studies

liposome	filter pore size (nm)	method of preparation	vesicle diameter (nm)
SUV	NA	sonication	44.2 ± 2
LUV_{100}	100	extrusion	119 ● 3
MLV_{400}	400	extrusion	244 ± 42

Preparation of Vesicles. Donor vesicles of EPC/sterol/Cer (75:10:15 mole ratio) with trace [^{3}H]CS or [^{3}H]-cholesterol and acceptor vesicles of EPC labeled with [^{14}C]CHE as a nonexchangeable marker were taken from lipid stock solutions in benzene/methanol (70:30 v/v) and lyophilized to ensure homogeneous mixing of all lipid components. A second set of donor vesicles, of the same composition, but labeled with [^{3}H]CHE, were made for use in parallel experiments designed to monitor the efficiency of vesicle separation after each incubation. Yet another preparation labeled with [^{3}H]CHE was used in ion-exchange chromatography. These experiments demonstrate the loss of surface negative charge in donor vesicles during incubations with acceptors (see methods below). Acceptor vesicles were prepared as above and were composed of EPC.

After lyophilization, the lipid mixtures were hydrated to a concentration of 10 mM with 150 mM NaCl, 20 mM HEPES, pH 7.4 (HEPES-buffered saline), and vortexed to generate MLV. LUV and oligolamellar vesicles were prepared by extruding the MLV 10 times through two stacked polycarbonate filters of 100 nm and 400 nm pore size, respectively, using a water-jacketed thermobarrel Extruder (Lipex Biomembranes, Vancouver, B.C.). SUV of approximately 40 nm diameter were prepared by sonicating MLV for two 15 min cycles using a Branson tip sonifier. The SUV were centrifuged at 10,000*g* for 30 min in an Eppendorf benchtop centrifuge to remove titanium fragments originating from the sonicator tip.

Determination of Vesicle Diameters. The diameters of vesicles generated by sonication and extrusion procedures were determined by quasi-elastic light-scattering (QELS) analyses utilizing a Nicomp Model 370 submicron laser particle sizer (Pacific Scientific, MD) equipped with a 5 mW helium−neon laser. The Nicomp QELS measures fluctuations in light-scattering intensities due to vesicle diffusion in solution. The calculated diffusion coefficient is used to obtain the average hydrodynamic radius and thus the mean diameter of vesicles. Table 1 shows the diameter of the three vesicle preparations expressed as the mean ± standard deviation. For reasons of clarity, throughout this report vesicles prepared by extrusion are referred to by the filter pore size used in their preparation. For example, LUV sized through 100 nm pore size filters are written as LUV_{100}, and MLV extruded through filters of 400 nm diameter are referred to as MLV_{400}.

Measurement of [^{3}H]Sterol Exchange. The rates of exchange of the [^{3}H]sterol from donor to acceptor vesicles

at 37 °C were measured by separating the two vesicle populations at different time intervals and after quantitating the level of radioactivity in the acceptors. Separation was achieved using the lectin binding method as described by Kan et al. (1992) with the following modifications. Briefly, donor vesicles containing sterol and *N*-palmitoyldihydrolactocerebroside were mixed with a 10-fold excess concentration of acceptors. Aliquots (50 μL) of this mixture were then placed in 1 mL Eppendorf tubes and diluted to 200 μL total volume with HBS to prevent evaporation. At specific time intervals, tubes were removed, 50 μg of lectin in phosphate buffer was added, the tubes were vortexed, and the mixtures were centrifuged for 3 min at room temperature to separate the lectin-aggregated donors from EPC acceptors. Aliquots (100 μL) of the supernatant containing the acceptors were transferred to scintillation vials, and 5 mL of Pico-Fluor scintillant was added prior to counting for 2 min in a Beckman LS 3801 liquid scintillation counter equipped with a [^{3}H]/[^{14}C] dual-label counting program.

In this type of analysis, it is critical to be able to account for not only the recovery of acceptors but also the small, time-dependent spillover of donors into the acceptor pool caused by the slow exchange of cerebroside. Here such a correction is possible because the lipid label used to follow vesicles (CHE) does not exchange on the time scale of these experiments. The recovery of acceptor vesicles was typically >85% and was monitored by measuring the [^{14}C]CHE counts present in the labeled EPC acceptor vesicles. Contamination by donor vesicles was assessed in experiments run parallel to the exchange measurements using donor vesicles labeled with [^{3}H]CHE and acceptors with [^{14}C]CHE. At early time points, it was noted that >98% of donor vesicles were precipitated after the addition of lectin. However, at progressively longer incubation times, for example, >16 h, approximately 10% of the donors could be detected in the supernatant.

The fraction of labeled cholesterol appearing in the acceptor LUV after each incubation interval was determined by calculating the percent sterol that underwent exchange and correcting for recovery of acceptor vesicles and donor vesicle contamination as follows:

$$X_a = \left\{\frac{[^3H]_t}{[^3H]_{mix}}\frac{[^{14}C]_{mix}}{[^{14}C]_t}\right\}_{sterol} - \left\{\frac{[^3H]_t}{[^3H]_{mix}}\frac{[^{14}C]_{mix}}{[^{14}C]_t}\right\}_{CHE} \quad (1)$$

where $[^3H]_t$ represents [^{3}H]sterol present in the supernatant (i.e., transferred to the acceptors) or [^{3}H]CHE associated with the donors used in the parallel experiments at any time t after separation and $[^3H]_{mix}$ represents [^{3}H]sterol or [^{3}H]CHE in the initial donor and acceptor mixture at $t = 0$ prior to separation. Similarly, $[^{14}C]_t$ represent counts remaining in the supernatant as acceptors after separation of the incubation mixture at time t during the sterol exchange experiments or as acceptors remaining in the parallel [^{3}H]CHE-labeled donor experiments. $[^{14}C]_{mix}$ represents the total [^{14}C] counts in the donor and acceptor mixtures prior to separation.

Calculation of Rate Constants for Transbilayer Diffusion and Exchange. The rate constants for exchange of cholesterol and CS from donor to acceptor vesicles (Figure 2A) were determined according to a three compartment model (described in Figure 2B). Compartments A and B represent the inner and outer monolayer of the donor vesicles, and

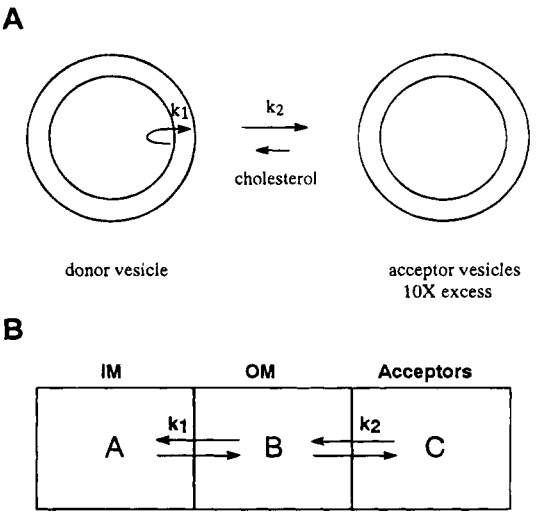

FIGURE 2: Experimental conditions, rate constants, and the three-compartment model. (A) Schematic representation of the experimental conditions and rate constants associated with the exchange process, k_1 (transbilayer migration) and k_2 (exchange). (B) Schematic representation of the three-compartment model. Compartments A and B represent the inner and outer monolayer of the donor vesicles and compartment C represents the acceptor bilayer.

compartment C, the bilayer of acceptor vesicles. The rate constant k_1 is assigned for the transbilayer movement from A to B and the rate constant k_2 for exchange from the outer monolayer of the donors (B) to the acceptors (C).

Flux equations that describe the change in the number of cholesterol or CS molecules in each compartment over time are described below. The change over time in the number of moles of sterol in each compartment is proportional to the difference in concentration of sterol in that compartment and adjacent compartments. Therefore:

$$\frac{dN_a}{dt} = k_1\left(\frac{N_B}{V_B} - \frac{N_A}{V_A}\right) \quad (2)$$

$$\frac{dN_B}{dt} = k_1\left(\frac{N_A}{V_A} - \frac{N_B}{V_B}\right) + k_2\left(\frac{N_C}{V_C} - \frac{N_B}{V_B}\right) \quad (3)$$

$$\frac{dN_C}{dt} = k_2\left(\frac{N_B}{V_B} - \frac{N_C}{V_C}\right) \quad (4)$$

N denotes the number of moles of sterol in each compartment (A, B, C), and V denotes the volume of each compartment (A, B, C). If Δt that are sufficiently small are used, then we can approximate dt by Δt, and thus the equations can be rewritten as

$$\Delta N_A = k_1\left(\frac{N_B}{V_B} - \frac{N_A}{V_A}\right)\Delta t \quad (5)$$

$$\Delta N_B = k_1\left(\frac{N_A}{V_A} - \frac{N_B}{V_B}\right)\Delta t + k_2\left(\frac{N_C}{V_C} - \frac{N_B}{V_B}\right)\Delta t \quad (6)$$

$$\Delta N_C = k_2\left(\frac{N_B}{V_B} - \frac{N_C}{V_C}\right)\Delta t \quad (7)$$

Instead of analytically solving equations 5, 6, and 7, a computer program written in GWBasic was used to numeri-

cally integrate and fit the experimental data of N_C and solve the simultaneous differential equations 5, 6, and 7 for each time interval (Δt). The curve-fitting program was used to determine the rate constants k_1 and k_2 that would best fit the experimental N_C values (percent sterol transferred to acceptors).

All cholesterol exchange experiments were performed with at least three different sets of donor and acceptor vesicles in separate experiments with duplicate measurements made at the time points indicated. These data are expressed as the mean ± standard deviation of data collected from all the experiments.

Estimation of the Amount of Lipid Present in the Outer Monolayer of Vesicles. MLV_{400} composed of EPC were prepared in HEPES-buffered saline as described above. The proton-decoupled 81.0 MHz ^{31}P-NMR spectra of vesicles before and after the addition of 5 mM manganese (Mn^{2+}) were recorded employing a Bruker MSL 200 spectrometer. The free induction decay (FID) was collected using a pulse width of 2.9 μs (25 °C) with an interpulse delay of 1.0 s. After 100 scans, the FID was Fourier-transformed using a line-broadening function of 25 Hz for the MLV_{400} and 10 Hz for the LUV_{100} and SUV. The Mn^{2+} added was impermeable to vesicles yet sufficient to broaden beyond detection the ^{31}P-NMR signal from phospholipid molecules facing the external medium. Spectra before and after Mn^{2+} quenching were printed, then cut and weighed to give an estimate of the percent phospholipid present in the outer monolayer of donor vesicles.

Ion-Exchange Chromatography of Vesicles Containing Cholesterol Sulfate. Donor vesicles composed of EPC/CS (90:10) or EPC/DSPG (95:5) and labeled with 1.0 μCi of [^{3}H]CHE were prepared as described previously and incubated at 37 °C with a 10-fold excess of EPC acceptors labeled with 0.1 μCi of [^{14}C]CHE. At the time intervals indicated, 0.5 mL aliquots of the mixtures were removed and the two vesicle populations separated on the basis of charge employing a 1 × 10 cm DEAE-Sepharose CL-6B column equilibrated with 50 mM NaCl, 20 mM HEPES (low-salt buffer). Initially, 1 mL fractions were collected using low-salt buffer, then a further 15 fractions were collected while eluting with high-salt, low-pH buffer (1 M NaCl, 20 mM citrate, pH 2.0). The elution profiles of both [^{3}H]CHE- and [^{14}C]CHE-labeled vesicles from the column are represented as the percent recovery of the total counts added.

RESULTS

SUV, LUV_{100}, and MLV_{400} exhibit markedly different ratios of surface area to total membrane, consequently, for the kinetic analyses, it was important to obtain accurate estimates of the pool sizes described in Figure 2B.

Compartment Volumes and Lipid Distributions. Of the three preparations, only SUV and LUV_{100} are known to be unilamellar (Hope et al., 1986); therefore, the phospholipid compartment for these vesicles can be divided into inner monolayer (IM) and outer monolayer (OM). MLV_{400}, on the other hand, are known to have an ill-defined number of internal lamellae. However, using ^{31}P-NMR, it was possible to accurately determine the amount of phospholipid in the surface monolayer and therefore also the IM of the external bilayer plus internal bilayers.

The volumes of compartments A and B, which represent the donor vesicle IM and OM, respectively, were calculated from the mean vesicle diameter (measured by QELS) and assuming an average phospholipid surface area of 0.6 nm^2 and a bilayer thickness of 5 nm. For the SUV preparation used in these studies (44 nm diameter), this yielded a volume for compartment A that was 42% of the total bilayer volume whereas the OM (compartment B) occupied 58% of the total volume. In all experiments, the phospholipid concentration of acceptor vesicles was 10-fold higher than that of the donors. In the SUV (donor), LUV (acceptor) system, the number of donor vesicles is approximately equal to the number of acceptors, because of the small diameter of the SUV; consequently, there was 1.08 times more SUV donor than LUV_{100} acceptor particles despite the latter being 10-fold excess with respect to phospholipid concentration. However, under these conditions, the volume of compartment C is 8.6 times the volume of B. For the LUV (donor), LUV (acceptor) experiments, the volume of C was 10-fold greater than B, and the number of acceptor vesicles was also 10-fold more than donors.

MLV sized through filters with a pore size of 400 nm have been shown by freeze−fracture to contain internal bilayers (Hope et al., 1986, 1989a). Consequently, simple geometric calculations cannot be used to estimate the IM and OM pool sizes. However, ^{31}P-NMR can be used to measure the amount of phospholipid in the external monolayer of the outer bilayer. Figure 3 shows the ^{31}P-NMR spectrum of MLV_{400} recorded before and after the addition of 5 mM Mn^{2+}. Figure 3A represents the phosphorous signal from all the phospholipids in the sample. The Mn^{2+} ion broadens the signal obtained from the phospholipid headgroup to such an extent that it does not contribute to the signal intensity measured under these conditions. The MLV_{400} are also impermeable to this ion; consequently, in the presence of Mn^{2+}, the signal intensity detected arises from only phospholipid located in the IM of the outer bilayer and any internal bilayers. Therefore, the difference in the integrated areas of spectra shown in Figure 3A and Figure 3B is equivalent to the proportion of total phospholipid in the OM of the MLV_{400} preparation, and was determined to be 40% of the total. Therefore, 80% of the total phospholipid is present in the external bilayer of this oligolamellar system, and the remaining 20% of phospholipid is located in internal lamellae. For the kinetic analyses, compartment A was assumed to be 60% of the total donor lipid (IM plus internal bilayers), and compartment B (OM) as 40%. Therefore, in the MLV_{400} (donor), LUV_{100} (acceptor) experiments, compartment C was calculated to be 10.4 times greater than B, but the ratio of MLV_{400} to LUV_{100} vesicles was 1:44.

Effect of Liposome Size and Lamellarity on Cholesterol Exchange. The exchange of cholesterol from three types of donor vesicles to acceptor vesicles is shown in Figure 4. Over the 24 h time course shown, cholesterol is available for exchange from all three liposomal systems, but in agreement with prior literature, the rates of exchange appear to decrease significantly with increasing vesicle size. This is illustrated in Table 2 which summarizes the rates of transbilayer movement (k_1) and exchange (k_2) for cholesterol and CS. Using the curve-fitting procedure described under Materials and Methods, a series of k_1 and k_2 values were tested and compared to values for N_C entered into the program for a given time t, until the best fit of all eight N_C data points was reached and values for k_1 and k_2 were derived.

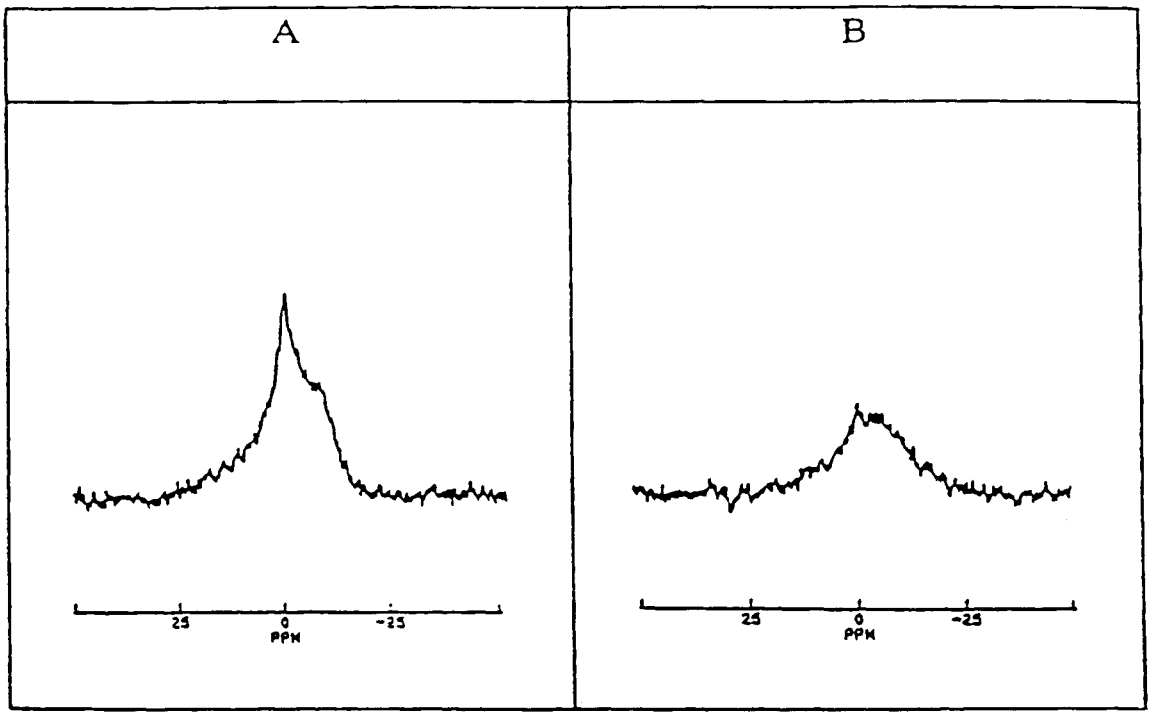

FIGURE 3: Estimation of outer monolayer phospholipid in MLV_{400}. (A) ^{31}P-NMR spectra of MLV_{400} composed of EPC before and (B) after the addition of manganese. From the difference in signal intensity, it was estimated that 40% of the total phospholipid was located in the OM of the external bilayer.

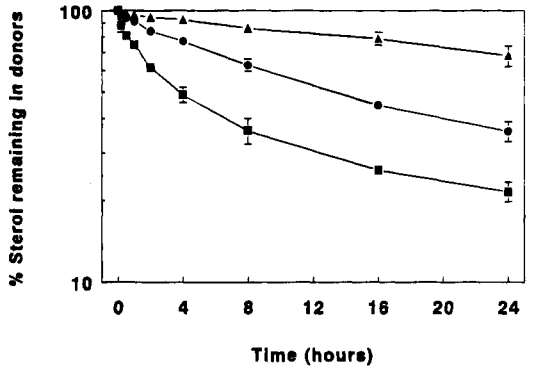

FIGURE 4: Movement of cholesterol between donor and acceptor vesicles. SUV (■), LUV_{100} (●), and MLV_{400} (▲) donors composed of EPC/CHOL/Cer (75:10:15) were incubated with a 10-fold excess concentration of EPC LUV_{100} at 37 °C in Eppendorf tubes. At the indicated times, the two vesicle populations were separated by centrifugation after the addition of 50 μg of galactosyl binding lectin. Subsequently, the percent cholesterol transferred to the acceptors was determined after quantitating by scintillation counting an aliquot of the supernatant which contains the acceptors. Data points represent the mean ± standard deviation (error bars) of all experiments described under Materials and Methods.

SUV, LUV_{100}, and MLV_{400} were found to exhibit an apparent half-time ($t_{1/2}$) for cholesterol exchange of 2, 4, and 12 h, respectively. In addition, we estimate the $t_{1/2}$ for transbilayer movement of cholesterol to be approximately 9 h in SUV and 12 h in LUV_{100}. The observation that the rate of cholesterol flip-flop in LUV_{100} is slower than in SUV may be due to the decreased rate of desorption of cholesterol from the OM of the larger vesicles, assuming that the IM and OM concentrations of cholesterol are in equilibrium. The rate of transbilayer movement for cholesterol in MLV_{400} cannot be determined accurately owing to the sterol exchange expected to occur with the internal lamellae. Using the three-compartment model, a k_1 is obtained which gives rise to a $t_{1/2}$ for flip-flop of more than 38 h, however, this k_1 value represents a hybrid rate constant accounting for transbilayer diffusion from internal lamellae and would therefore overestimate the true rate of transbilayer diffusion.

The kinetic model employed predicts that the transbilayer diffusion of sterol is slower than the rate of desorption from the OM for all three liposomal systems examined. Consequently, under nonequilibrium conditions favoring net cholesterol flux from donor to acceptor, the OM cholesterol concentration will decrease more quickly than the IM concentration. This is shown graphically in Figure 5, panels A–C. Using the k_1 and k_2 values calculated for the three liposomal systems, the cholesterol content of the OM (solid squares) and IM (solid triangles) and the total cholesterol remaining in donors (solid circles) are shown. For SUV, it is estimated that approximately 75% of the cholesterol located at the OM is removed within 4 h, whereas only 15% of the IM sterol pool has been reduced (Figure 5A). Similarly, for LUV_{100}, about 50% of the OM cholesterol has been depleted at 4 h compared to less than 10% from the IM (Figure 5B). The exchange process is much slower for MLV_{400}; nevertheless, after 24 h, more than 60% of the sterol in the OM has been removed, but only 15% of the sterol from the IM and internal bilayers is depleted (Figure 5C).

Effect of Liposome Size and Lamellarity on Cholesterol Sulfate Exchange. In the previous section, it was found that the kinetics of cholesterol exchange could be described by a model in which the rate of diffusion of sterol from the IM to OM was slower than the rate of cholesterol exchange from donor to acceptor vesicles. Here the kinetics for CS exchange are described using the same experimental procedures and model. As predicted, the differences between k_1 and k_2 are much greater than those observed for cholesterol. As shown in Figure 6, CS exchange occurs very rapidly during the first 4 h of incubation. The rate constants (see

Table 2: Summary of Rate Constants and Half-Times for Flip-Flop and Exchange in Various Sized Vesicles

donor liposome	initial pool size (IM/OM)	cholesterol				cholesterol sulfate			
		k_1	$t_{1/2,flip}$ (h)	k_2	$t_{1/2,exc}$ (h)	k_1	$t_{1/2,flip}$ (h)	k_2	$t_{1/2,exc}$ (h)
SUV	42/58	0.075	9.2	0.44	1.6	0.043	16.1	3.41	0.20
LUV_{100}	50/50	0.058	12.0	0.18	3.9	0.047	14.8	1.12	0.62
MLV_{400}	60/40	0.018	38.3	0.057	12.2	0.046	15.1	0.51	1.36

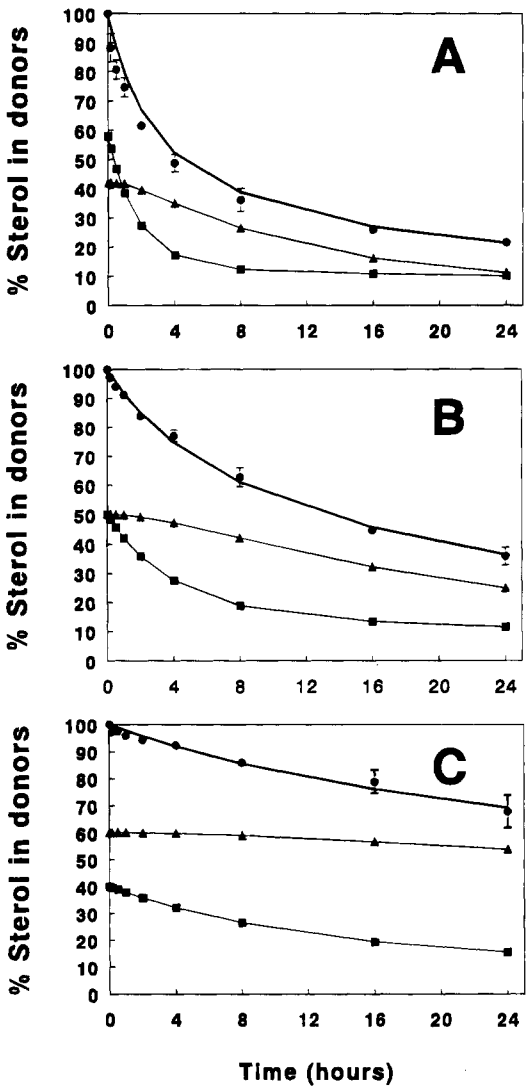

FIGURE 5: Depletion of cholesterol from the IM and OM estimated by the kinetic model. The percent sterol remaining in donor vesicles of various size following their incubation with a 10-fold excess of acceptors is redrawn as (●). The line tracing the points represents the best fit of the data using the three-compartment model described (Materials and Methods). In addition, the estimated contribution of the inner (▲) and outer (■) monolayer sterol is shown. The analysis was carried out for (A) SUV donors, (B) LUV_{100} donors, and (C) MLV_{400} donors. Data points represent the mean ± standard deviation (error bars) of all experiments described under Materials and Methods.

Table 2) give rise to an exchange $t_{1/2}$ of 0.2 h for SUV, nearly an order of magnitude faster than that observed for cholesterol in the same vesicles. The rate of exchange is similarly enhanced from LUV_{100} and MLV_{400}. These data are consistent with the reduced energy required for CS to desorb from the surface of the OM due to the presence of the hydrophilic sulfate moiety.

It is also clear from the data shown in Figure 7 that the kinetics for CS are more obviously biphasic than those seen

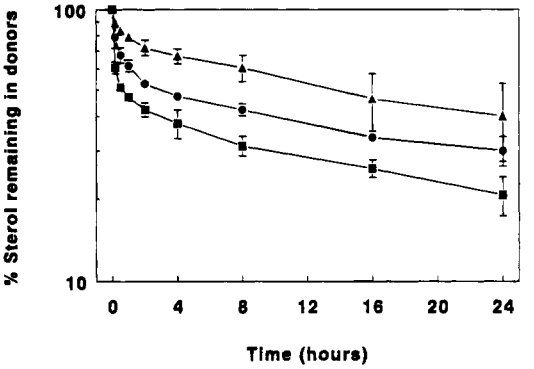

FIGURE 6: Movement of cholesterol sulfate between donor and acceptor vesicles. SUV (■), LUV_{100} (●), and MLV_{400} (▲) donors composed of EPC/CS/Cer (75:10:15) were incubated with a 10-fold excess concentration of EPC LUV_{100} at 37 °C in Eppendorf tubes. At the indicated times, the two vesicle populations were separated by centrifugation after the addition of 50 μg of galactosyl binding lectin. Subsequently, the percent CS transferred to the acceptors was determined after quantitating by scintillation counting an aliquot of the supernatant which contains the acceptors. Data points represent the mean ± standard deviation (error bars) of all experiments described under Materials and Methods.

for cholesterol (Figure 5). The three-compartment model was used to obtain k_1 (transbilayer rate) and k_2 (exchange rate) for CS (Table 2). It is interesting to note that the rate of CS flip-flop in SUV and LUV_{100} is slower than that estimated for cholesterol, as predicted; however, the difference is not as large as that observed in the rate of exchange between vesicles. When concentrations of CS in the IM and OM are plotted against time then the exaggerated difference between k_1 and k_2 is highlighted. As shown in Figure 7, within 1 h, >80% of CS in the OM of SUV has been removed, while <5% of sterol from the IM has been depleted. A slower flux is seen from LUV_{100}, but by 2 h, a similar sterol transbilayer asymmetry has been induced.

Although the kinetic model predicts that an asymmetric distribution of cholesterol also exists due to the depletion process, this cannot be readily confirmed by other techniques. However, because CS is negatively charged (pK_a < 2; data not shown) at the pH of these experiments, it is possible to detect changes in distribution by monitoring the decrease in surface charge of the vesicles as CS is depleted from the OM and diffuses into acceptors. Using LUV_{100} donors and a 10-fold excess of acceptors, ion-exchange chromatography was employed to show that after 4 h the surface charge of donors was greatly reduced. We have employed this technique before to measure changes in vesicle surface charge (Hope & Cullis, 1987; Hope et al., 1989b; Eastman et al., 1992). Elution profiles are shown in Figure 8. Neutral EPC LUV_{100} elute from the DEAE-Sepharose column in the void volume (Figure 8A) whereas vesicles composed of EPC/CS (90:10 mole ratio) adhere to the positively charged Sepharose and can only be eluted at high ionic strength and low pH, as shown in Figure 8B. However, after 4 h incubation with acceptor vesicles, the LUV_{100} containing CS

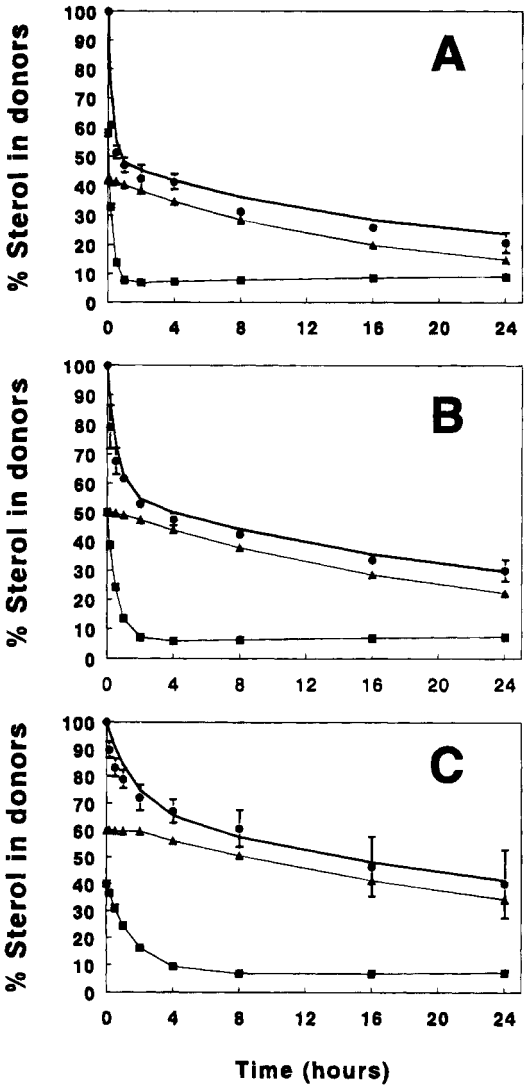

FIGURE 7: Depletion of cholesterol sulfate from the IM and OM estimated using the kinetic model. The kinetics of cholesterol sulfate transfer to acceptor vesicles are redrawn as (●). The line tracing the points represents the best fit of the data using the three-compartment model described (Materials and Methods) In addition, the estimated contribution of the inner (▲) and outer (■) monolayer sterol is shown. The analysis was carried out for (A) SUV, (B) LUV_{100}, and (C) MLV_{400}. However, the IM cholesterol for MLV_{400} includes approximately 20% of the total lipid trapped as internal lamellae donors. Data points represent the mean ± standard deviation (error bars) of all experiments described under Materials and Methods.

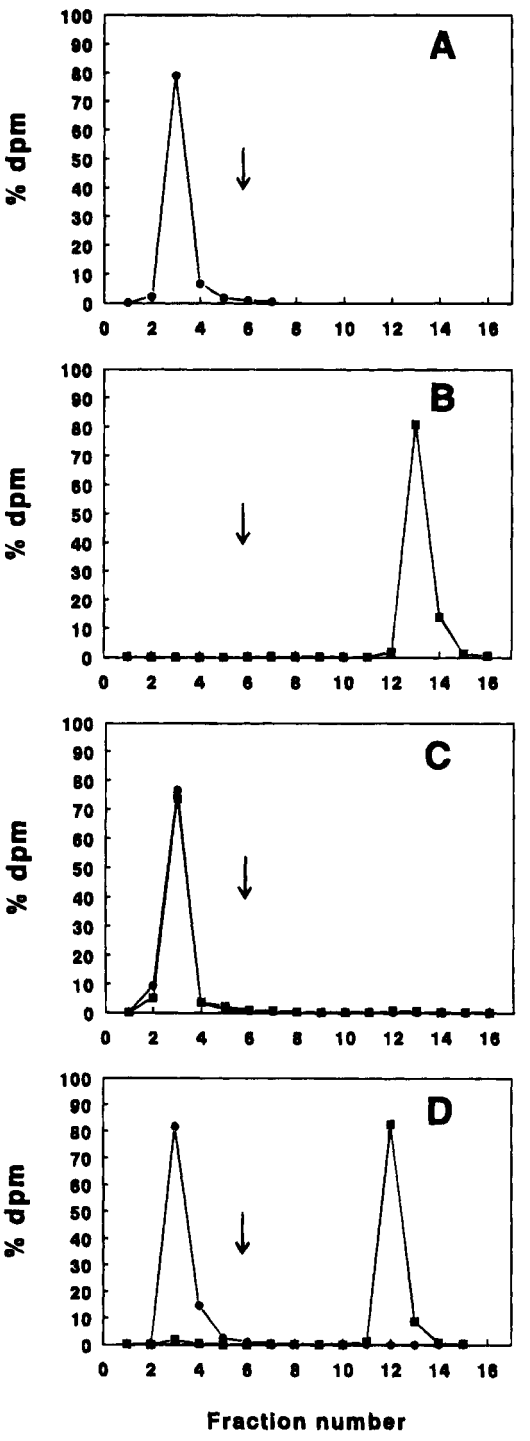

FIGURE 8: Elution of vesicles from DEAE-Sepharose columns: measurement of surface charge. Elution profiles from DEAE-Sepharose columns of (A) EPC acceptors (●), labeled with trace [^{14}C]CHE, (B) EPC/CS (90:10) donors (■), labeled with trace [^{3}H]-CHE, (C) a mixture of A (●) and B (■) after 4 h incubation at 37 °C, and (D) a mixture of EPC acceptors (●) and EPC/DSPG (95:5) (■), after 4 h incubation at 37 °C. The arrow indicates the point at which elution with high-salt, low-pH buffer was initiated.

now elute in the void volume (Figure 8C), suggesting that they have lost their surface negative charge, which is consistent with the data shown in Figure 7B, indicating that the OM contains <6% of its original concentration of CS, even though at 4 h only 50% of the total CS contained in the vesicles has been depleted.

In order to demonstrate that simply reducing the negative surface charge by 50% is not sufficient to prevent vesicles from binding to the ion-exchange column, a parallel experiment was performed using donor vesicles composed of EPC/DSPG (95:5 mole ratio). The negatively charged phospholipid (DSPG) does not exchange under the incubation conditions employed. As can be seen, in Figure 8D, these vesicles remain bound to DEAE-Sepharose until eluted with high ionic strength and low pH, even after 4 h of incubation with a 10-fold excess of acceptors.

It is interesting to note that the $t_{1/2}$ for transbilayer diffusion of CS in MLV_{400} is similar to that observed for the unilamellar systems (see Table 2). Although the reasons for this are not clear, it is likely that the MLV_{400} containing CS have fewer, if any, internal lamellae due to the presence of negative surface charge (Hope et al., 1986). This hypothesis is supported by the observation that cholesterol donors of

MLV_{400} containing 10 mol % EPG also exhibit faster k_1 than systems that do not contain PG (data not shown).

DISCUSSION

The kinetics of cholesterol exchange between model membrane systems have been studied extensively [see Phillips et al. (1987) and refernces cited therein]. The variation between the rates of exchange reported in the literature is large, even when differences in donor size and composition are considered. For example, SUV represent "limit size" vesicles (Hope et al., 1986) usually made in the laboratory by the same process (sonication) and should therefore represent a vesicle population that exhibits similar physical characteristics that can be consistently generated by all research groups. However, the literature data referring to cholesterol movement from donor SUV, composed of phospholipid in the liquid-crystalline state at the experimental temperature, fall into three categories. First, several groups (Dawidowicz & Backer, 1981; Backer & Dawidowicz, 1979; Kan & Bittman, 1991; McLean & Phillips, 1981, 1984; Nakagawa et al., 1979; Bloj & Zilversmit, 1979; Thomas & Poznansky, 1988; Fugler et al., 1985) have shown that exchange can be modeled by a single exponential and report complete exchangeability of cholesterol from donors. These kinetics were observed under equilibrium (exchange) and nonequilibrium (net transfer) conditions. The second category is represented by data showing the presence of a small pool of nonexchangeable cholesterol which appears thermodynamically "locked" within the bilayer. Poznansky and Lange (1978) found approximately 10−20% of cholesterol did not participate in exchange under equilibrium conditions, and Bar et al. (1986) noted a similarly sized pool did not transfer to acceptors in studies employing nonequilibrium conditions. The third category describes exchange and net flux kinetics in which two exchangeable pools of cholesterol are observed. These exchange data can be best fit as a function of two exponentials (Nemecz et al., 1988) and have been interpreted as representing either two pools of sterol, one in the OM and the other at the IM (Poznansky & Lange, 1978), or laterally segregated areas of the membrane that posses different C:P ratios which exhibit different rates of exchange (Bar et al., 1986; Nemecz et al., 1988; Schroeder et al., 1991).

Here we have employed three different, but well-characterized, model membrane donors and compared the net transfer kinetics of cholesterol and CS to the same LUV-type acceptor. CS is a naturally occurring derivative of cholesterol, which interacts with phospholipids in a manner similar to that observed for cholesterol (Kitson et al., 1992). The three-compartment model used to analyze the flux data presented in this study assumes that at $t = 0$ the transbilayer distribution of cholesterol is such that the C:P ratios of the IM and OM of the donors are equal. This is consistent with the known dynamics of cholesterol in model membrane systems that do not exhibit phospholipid asymmetry (Newman & Huang, 1976; Hyslop et al., 1990). We found that the data obtained for both lipids were best described by two rate constants, k_1 represented the rate of transbilayer diffusion from the IM to OM of donors and k_2 the diffusion of sterol from the OM to excess acceptor membrane. However, the overall rate of cholesterol efflux from donor vesicles was found to be comparable to those reported in the literature. Furthermore, when data reporting a single pool of cholesterol were drawn from the literature and analyzed using the model described here, cholesterol efflux rates were very similar to those reported, and a k_1 value for the best fit was not detected.

As we predicted, the biphasic behavior of CS was better defined than that obtained for cholesterol. Furthermore, the rapid decrease in surface charge observed for vesicles containing CS is consistent with the hypothesis that the fast and slow exchanging components represent sterol located in the OM and IM, respectively. The efflux from the OM to acceptors (k_2) is almost 2 orders of magnitude faster than flip-flop (k_1) in SUV and LUV, resulting in nearly complete depletion of CS from the OM at incubation times when only 50% of the initial CS content has transferred to acceptors (Figure 7). The resulting asymmetric distribution of CS is reflected by the elution of these donors from ion-exchange columns, indicating a reduction in surface charge greater than would be observed if the remaining CS was equally distributed across the bilayer.

Kan et al. (1992) have recently shown that the rate of sterol exchange between membranes is dependent on sterol structure. Synthetic analogues of cholesterol that are more hydrophilic generally exhibit faster rates of exchange. Moreover, in contrast to their observations for cholesterol, biphasic kinetics were observed for zwitterionic sterols and sterols bearing a positive charge at carbon 3. These authors suggest that the slow phase kinetics reflect the higher energy required to move charged sterols from the inner to outer leaflet of the bilayer. The results presented here for CS are consistent with their observations.

Although our cholesterol flux data can also be described as biphasic, it is not possible to monitor the OM concentration of the neutral sterol during depletion. Consequently, we are unable to distinguish between a model in which the slowly exchanging pool represents IM cholesterol and one where laterally segregated domains exist in the OM, which exhibit different C:P ratios and different rates of efflux (Schroeder et al., 1991). Phase diagrams of cholesterol and phospholipids in a bilayer have been made, showing the existence of lateral domains between 5 and 30 mol % cholesterol, the range used in these studies (Darke et al., 1972). On the other hand, the existence of lateral domains which exhibit different concentrations of cholesterol within the plane of liquid-crystalline, biological membranes remains contentious. It has been argued that the rates of rotation and diffusion of lipid molecules within a fluid bilayer are too fast for restrictive interactions between phospholipids and cholesterol to affect lateral distribution (Yeagle, 1981; Miller, 1984). In addition, Hyslop et al. (1990), using fluorescence intensity and lifetime measurements of cholestatrienol (a cholesterol analogue that exhibits similar behavior to cholesterol), could only detect a homogeneous distribution of the reporter molecule over a range of sterol to phospholipid molar ratios.

The apparent rates of transbilayer movement calculated for cholesterol in this study are considerably slower than those reported by others [see Schroeder and Nemecz (1990) for a review]. However, flip-flop rates on the order of several hours could explain the existence of "non-exchangeable" pools of cholesterol observed by several groups who only measured kinetics for 8 h (Bar et al., 1986, 1987). If the rate of cholesterol transbilayer movement is indeed on the order of hours, then in order to examine the exchangeability of cholesterol, data would have to be collected for at

least several half-times of transbilayer diffusion to approach equilibrium. This point has also been noted by Kan and Bittman (1991), who showed that if cholesterol efflux data are monitored until equilibrium is approached then the size of the nonexchangeable pool is decreased.

Nevertheless, it remains unclear why phospholipid vesicles composed of very similar phospholipid and cholesterol content exhibit such different kinetics in both the rate and extent of cholesterol exchange. One explanation could be vesicle size variations resulting from the different lipid compositions employed. For example, vesicles increase in size with increasing cholesterol content, even when made by the same process. Another possibility is the the extent to which donor and acceptor vesicles have been separated following an incubation (Nemecz & Schroeder, 1988). As a result of slow exchange of lipid, incorporated to distinguish the two populations, donor/acceptor separation progressively diminishes over time; consequently, spillover detected during later time points may skew the results. In order to account for this in our studies, experiments using a nonexchangeable marker were run in parallel and the data used to correct for donor contamination. Without this correction, the data for cholesterol would have fit a single-exponential function. This point has been made by others who have noted a nonexchangeable pool of cholesterol (Poznansky & Lange, 1976; Bar et al., 1986). Backer and Dawidowicz (1979) claimed that MLV contamination of SUV preparations is responsible for the observation of nonexchangeable pools, however, other groups disagree (Poznansky & Lange, 1978; Bar et al., 1986).

Finally, it is of interest to note the large difference in exchange behavior of CS and cholesterol. The biological role of CS is unknown, and so it is difficult to speculate as to whether the exchange kinetics observed for this sterol serve a functional purpose *in vivo*. Quantitatively, CS is most abundant in the epidermis, where it is synthesized by cholesterol sulfotransferase (Elias et al., 1984), and is an integral part of the lipid composition of the outer layers of skin. It has been linked to desquamation, the natural process whereby corneocytes are sloughed from the surface of the skin. As terminally differentiated cells approach the skin surface, CS is hydrolyzed to cholesterol by cholesterol sulfatase (arylsulfatase C), which appears to promote desquamation. In a rare genetic disease in which cholesterol sulfatase is missing, excessive scaling occurs. Studies of this disease (recessive X-linked ichthyosis) have shown that desquamation is partly regulated by the ratio of CS to cholesterol in the stratum corneum, the outermost layer of skin (Williams, 1992). Normally this ratio is 1:500, whereas scaly skin can exhibit ratios as high as 1:5 (Lampe et al., 1983).

It is not clear how the differences in thermodynamic behavior between CS and cholesterol could be involved in maintaining skin structure. However, it is possible that the exchange properties of CS and cholesterol can be used therapeutically to decrease scaling in patients suffering from X-linked ichthyosis. Given the rapid exchange rate for CS, a topical application of unilamellar liposomes containing cholesterol might be expected to change the CS to cholesterol ratio of the stratum corneum, by removing excess CS as well as inserting exogenous cholesterol. There is evidence that scaling can be reduced by cholesterol replacement therapy (Feingold & Elias, 1993), suggesting that such a liposomal application could be therapeutically useful.

In summary, the data presented in this study clearly show that in three well-characterized model membrane systems the rate of CS flux from donors to acceptors is restricted by transbilayer diffusion of sterol from the IM to OM, so much so that almost complete asymmetry can be generated in donors where 50% of the remaining CS is localized to the IM. The best fit of our cholesterol data is also described by a model which assumes a rate constant for flip-flop that is slower than the rate of transfer from the OM to acceptors. However, it is not possible to distinguish between this and a model in which there are lateral domains within the plane of the bilayer that give rise to areas with different rates of cholesterol desorption (Nemecz & Schroeder, 1988).

ACKNOWLEDGMENT

We thank Dr. Steven Ansell for his assistance in the synthesis of cholesterol sulfate.

REFERENCES

Backer, J. M., & Dawidowicz, E. A. (1979) *Biochim. Biophys. Acta 551*, 260−270.
Backer, J. M., & Dawidowicz, E. A. (1981) *J. Biol. Chem. 256*, 586−588.
Bar, L. K., Barenholz, Y., & Thompson, T. E. (1986) *Biochemistry 25*, 6701−6705.
Bar, L. K., Barenholz, Y., & Thompson, T. E. (1987) *Biochemistry 26*, 5460−5465.
Bleau, G., Lalumiere, G., Chapdelaine, A., & Roberts, K. D. (1974) *Biochim. Biophys. Acta 352*, 1−9
Bligh, E. G., & Dyer, W. J. (1959) *Can. J. Biochem. Physiol. 37*, 911−917
Bloj, B., & Zilversmit, D. B. (1977) *Biochemistry 16*, 3943−3948.
Darke, A., Finer, E. G., Flook, A. G., & Phillips, M. C. (1972) *J. Mol. Biol. 63*, 265−279.
Dawidowicz, E. A., & Backer, J. M. (1981) *Biochim. Biophys. Acta 644*, 373−375.
Eastman, S. J., Hope, M. J., & Cullis, P. R. (1991) *Biochemistry 30*, 1740−1745.
Elias, P. M., Williams, M. L., Maloney, M. E., Bonifas, J. A., Brown, B. E., Grayson, S., & Epstein, E. H., Jr. (1984). *J. Clin. Invest. 74*, 1414−1421.
Feingold, K. R., & Elias, P. M. (1993) *Arch. Dermatol. 129*, 728−738.
Hope, M. J., & Cullis, P. R. (1987) *J. Biol. Chem. 262*, 4360−4366.
Hope, M. J., Wong, K. F., & Cullis, P. R. (1989a) *J. Electron Microsc. Tech. 13*, 277−287.
Hope, M. J., Redelmeier, T., Wong, K. F., Rodrigueza, W., & Cullis, P. R. (1989b) *Biochemistry 28*, 4181−4187.
Hope, M. J., Bally, M. B., Mayer, L. D., Janoff, A. A., & Cullis, P. R. (1986) *Chem. Phys. Lipids 40*, 89−107.
Hyslop, P. A., Morel, B., & Sauerheber, R. D. (1990) *Biochemistry 29*, 1025−1038.
Kan, C. C., & Bittman, R. (1991) *J. Am. Chem. Soc. 113*, 6650−6656.
Kan, C. C., Yan, J., & Bittman, R. (1992) *Biochemistry 31*, 1866−1874.
Kitson, N., Monck, M., Wong, K., Thewalt, J., & Cullis, P. (1992) *Biochim. Biophys. Acta 1111*, 127−133.
Lampe, M. A., Burligame, A. L., Whitney, J., Williams, M. L., Brown, B. E., Roitman, E., & Elias, P. M. (1983) *J. Lipid Res. 24*, 120−130.
Lund-Katz, S., Laboda, H. M., McLean, L. R., & Phillips, M. C. (1988) *Biochemistry 27*, 3416−3423.
Mayer, L. D., Hope, M. J., & Cullis, P. R. (1986) *Biochim. Biophys. Acta 858*, 161−168.
McLean, L. R., & Phillips, M. C. (1981) *Biochemistry 20*, 2893−2900.
McLean, L. R., & Phillips, M. C. (1982) *Biochemistry 21*, 4053−4059.

McLean, L. R., & Phillips, M. C. (1984) *Biochim. Biophys. Acta 776*, 21−26.
Miller, R. (1984) *Cell Biol. Int. Rep. 8*, 519−535.
Nakagawa, Y., Inoue, K., & Nojima, S. (1979) *Biochim. Biophys. Acta 553*, 307−319.
Nemecz, G., & Schroeder, F. (1988) *Biochemistry 27*, 7740−7749.
Nemecz, G., Fontaine, R. N, & Schroeder, F. (1988) *Biochim. Biophys. Acta 943*, 511−521.
Phillips, M. C. (1992) in *Structural and dynamic properties of lipids and membranes* (Cherry, R. J., & Quinn, P. J., Eds.) pp 103−118, Portland Press, London.
Phillips, M. C., Johnson, W. J., & Rothblat, G. H. (1987) *Biochim. Biophys. Acta 906*, 223−276.
Poznansky, M. J., & Lange, Y. (1976) *Nature 259*, 420−421.
Poznansky, M. J., & Lange, Y. (1978) *Biochim. Biophys. Acta 506*, 256−264.
Rehfield, S. J., Williams, M. L., & Elias, P. M. (1986) *Arch. Dermatol. Res. 278*, 259−263.
Schroeder, F., & Nemecz, G. (1990) in *Advances in cholesterol research.* (Esfahani, M., & Swaney, J., Eds.) pp 47−87, Telford Press, West Caldwell, NJ.
Schroeder, F., Jefferson, J. R., Kier, A. B., Knittel, J., Scallen, T. J., Wood, W. G., & Hapala, I. (1991) *Exp. Biol. Med. 196*, 235−252
Thomas, D. P., & Poznansky, M. J. (1988a) *Biochem. J. 251*, 55−61.
Thomas, D. P., & Poznansky, M. J. (1988b) *Biochem. J. 254*, 155−160.
Wertz, P. W. (1992) *Semin. Dermatol. 11*, 106−118.
Williams, M. L. (1992) *Semin. Dermatol. 11*, 169−175.
Yeagle, P. L. (1981) *Biochim. Biophys. Acta 640*, 263−273.

BI942627Y